

## Appendix A VSE-355G2/3 Testing Regime

A suite of tests were performed at South Mudd on the Caltech Campus (the location of CISN test station DSN), Kresge Lab in the nearby San Raphael Hills (PAS, PASA, PASB), and Robinson Building also on Caltech Campus (CRP, CRPA). We thank David Johnson, Jascha Polet, Wayne Miller, Mike Watkins and Robert Busby for their advice and help in performing the tests, and obtaining data.

Mr. Isamu Yokoi was the principal contact with Tokyo Sokushin. Mr. Masayuki Kurahashi and Mr Soturu Wada from Sokushin also participated in the testing.

A complete chronological presentation of the results from the cart tests, as well as other important data, is at [www.ecf.caltech.edu/~jclinton/vse/VSEtests.html](http://www.ecf.caltech.edu/~jclinton/vse/VSEtests.html).

### A.1 12 December 2001: DSN — Noise and Track Test

The VSE-355G2 was initially installed at CISN/TriNet test station DSN in the basement of S. Mudd, Caltech. The instrument was mounted on a milling machine alongside an EpiSensor, attached to a Quanterra Q736 data logger. On 12 December 2001 the 2 instruments were moved back and forth along the track of the milling machine, each length taking about 20s to run about 25cm. The objective of the test was to investigate the accuracy of displacement derived from the VSE-355G2, and compare it to that from the EpiSensor.

Unfortunately, over the length of the track, there was some minor tilt, which we discovered dominated the instrument output, and we could only conclude that the test served only to illustrate the sensitivity of the instruments to tilt. It was impossible to accurately determine displacement from this test. Both instruments recorded data that indicated a static offset in the SDOF mass, as seen in Figure A.1, sub-figures B and C. We were able to estimate the magnitude of the tilt from the static offset — in both cases this was found to be about  $0.0007\text{rads}$ , or  $0.04^\circ$ . This was enough to dwarf the relatively small translational displacement derived from each instrument, as is clearly seen in sub-figure B of Figure A.1.

We modeled the tilt as a step at the starting time of the milling machine displacement, which from sub-figures A and D of Figure A.1, is clearly only accurate in estimating final offset (seen in sub-figures B and C of Figure A.1), and not in modeling the motion recorded during the test themselves. In this case, the tilt is likely to occur non-linearly along the track, and is extremely difficult to model.

In sub-figure A of Figure A.1, the thick solid line represents the VSE-355G2 response to a  $\delta$ -function impulse in acceleration,  $V(t)$ , which is defined by Eqn. 3.20 in Section 3.2. A positive  $\delta$ -function at time  $t = 0s$  with a negative  $\delta$ -function at  $t \sim 22s$ . This is the expected result from the translational movement along the track - we assume an instantaneous rise to a constant velocity, and an instantaneous fall to rest (similar to Figure 3.9). The dashed-dotted line is the same, but includes the VSE-355G2 response to a step in acceleration (Eqn. 3.19, Figure 3.6) at time  $t = 0$ .

Sub-figure B is the integral of data in sub-figure A, representing the displacement of the VSE. We see a large constant offset of  $160cm$ . The size of the step in sub-figure A was chosen so as to match this final offset. The final displacement of the VSE-355G2 does indeed look like a sum of the acceleration step function (Figure 3.6) and a static offset in displacement (Figure 3.9).

Sub-figures C and D present the data from and simulation of the EpiSensor in the same test. A tilt is again required to map the offsets. The thick solid line again is the model without tilt, only with a  $\delta$ -function in acceleration at the beginning and end of the test. In this case response is given by Eqn 3.19, which is also the SDOF response to a  $\delta$ -function in acceleration. We use this here instead of Eqn 3.20 as the EpiSensor instrument has a displacement transducer, not a velocity transducer as with the VSE. Note the EpiSensor has a natural frequency of  $180Hz$  and is critically damped. The dashed-dotted line also includes a step in acceleration (Eqn 3.21). We note again a tilt is required to fit the permanent offset.

An investigation into the noise levels of the VSE-355G2 was made by comparing the sensor output with data from a co-located CMG-40T at DSN. Unfortunately, the site proved too noisy to measure instrument resolution, even when placed on a bed of sand. Some parasitic resonances at high frequencies ( $> 10Hz$ ) were observed. It was decided to move the instrument to a quieter location, and co-locate it with a better long-period instrument to

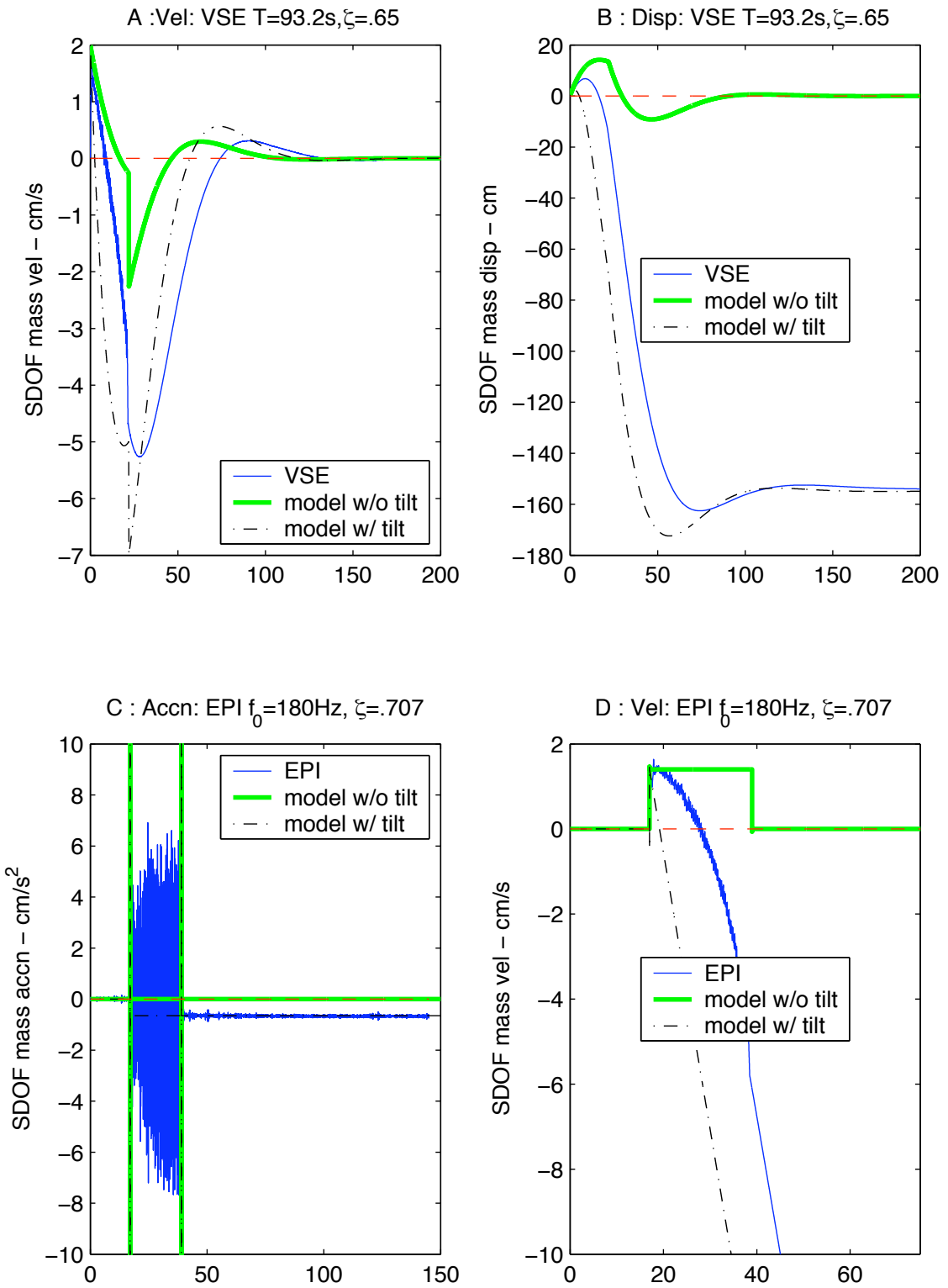


Figure A.1: Data and model from VSE-355G2 and EpiSensor: Milling machine test at DSN, December 2001.

better understand the frequency response.

## **A.2 February - March 2002: PASA — Noise and Screw Test**

The VSE-355G2 was moved to the nearby Kresge lab in the San Rafael Hills, site of the TriNet stations PAS, in order to better measure the noise floor of the instrument. It was installed about 10m from PAS (PAS is located in the inner vault at Kresge). It was recorded on a Q4128 as PASA, with an STS-2 (#99713) also being recorded on the digitiser located on the pier in the anteroom. On 4 March, 2002, we performed a ‘screw’ test, in which a levelling screw was twisted slightly, imparting a step in acceleration on the horizontal components of the instrument. This test was not successful, as in order to use the screw, we had to loosen a locked bolt at the instrument footing which imparted an instrument response into the transient, which had not fully damped out before we adjusted the levelling screw. Further, the twisting was not instantaneous, and it was difficult to model exactly. To rectify the first problem, a further screw test was performed on 7 March, 2002, in which the loosening of the bolt was performed the previous day. It was still difficult to model the resulting data with confidence, due to the transience of the twisting excitation which we modeled as a step. From this analysis it was clear that the calibration coil test would likely provide a more satisfactory estimate of the equivalent SDOF response. We also tried to adjust the levelling screw of the STS-2, but were unable to keep the instrument on scale. Figure A.2 shows the timeseries data from the 4 March screw test.

## **A.3 March 2002: PASB — Noise and Calibration Coil Test**

The VSE-355G2 was moved from the inner vault area to the ante-room at Kresge, and was placed on the pier alongside the STS-2 from the test above. Both instruments were recorded on the same Q4128 as before, and the station was renamed PASB. On 13 March, 2002,

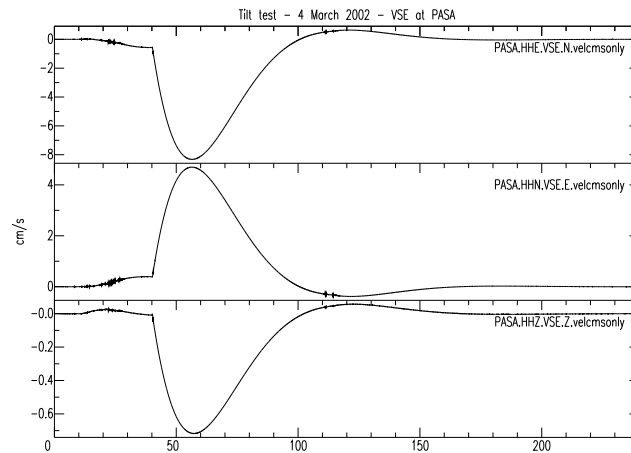


Figure A.2: Tilt test for VSE-355G2 using levelling screws in normal operation, from 4 March 2002. Unlocking of sensor, and transient tilting signal prove difficult to model exactly, so a calibration test was performed (see Figure 3.12). Contrast with tilt test performance for VSE-355G3 in November 2003 and January 2004 (Figures A.9 and A.12)

calibration tests for all 3 components of the VSE-355G2 were performed (see Figure 3.12). The calibration test involved applying a signal generated current in the form of a step function with a period of a few minutes to the calibration coil. It was observed during the test that unless we used much greater resistance than indicated in the Operation Manual, the system was over-driven (increasing the resistance decreases the applied current, which reduces the equivalent applied velocity). We noted that when smaller resistances were used, which effectively leads to larger output voltages, the clip occurred at about 600,000 *cts*, equivalent to 1.43 *Volts*, or a velocity of 14.3 *cm/s*. The clip velocity should be 2 *m/s*. Unfortunately none of the other mechanical tests performed so far (mill test, tilt test) had driven the instrument above this level, so at this stage we were unable to tell whether this was isolated to a problem with the calibration coil, or something that would affect the instruments ability to record motions up to 200 *cm/s* / 2 *g* (recall that the VSE sensor clips if either a maximum velocity or acceleration is recorded).

Seismic waveforms from some small local events were recorded, which were useful in calibrating the sensitivity of the instrument (see Figure 3.11), as well as noise data from

which we estimated the instrument's minimum resolution (see Figures 3.14, 3.15 and 3.16).

#### **A.4 8 March 2002: DSN — Cart Test I**

The VSE-355G2 was moved back to South Mudd. As there were some problems observed during the calibration test regarding saturation at Voltage significantly lower the published, it was decided to check whether, under real motion, the instrument was performing near its published capacity, which would make it capable of recording on-scale motions near  $2m/s$  and  $2g$ . On 8 March 2002, the instrument was placed on a cart alongside an EpiSensor, and attached to the Q4128 we operated as PASB above. We moved the cart up to  $10m$  along the floor at a range of speeds for durations of  $\sim 8s$ . We observed similar clipping at  $\pm 15cm/s$  or  $\pm 1.3V$  as in the calibration tests. Once the instrument reached this level, there would be a spike in velocity, then the instrument would 'flat-line' at  $15cm/s$  for some seconds. We performed multiple tests to ensure the spike was not at  $2m/s$  and then just fell back to  $15cm/s$ . Figure 3.21 illustrates this well, where the accelerometer data indicates the maximum velocity is at about  $60cm/s$ , and the VSE-355G2 does not nearly reach this level..

#### **A.5 June 2002: DSN — Cart Test II**

After correspondence with the manufacturer, the source of the low clipping was identified as a problem with the power regulator, which prevented the final stage amplifier from working correctly. The Vice-President of the company, Mr. Isamu Yokoi, visited Caltech on the 18<sup>th</sup> and 19<sup>th</sup> of June, 2002, to rectify the problem. Once this problem had been corrected, we repeated our cart test as described in the section above. The test showed improved performance, with excellent VSE correspondence with the EpiSensor data up to  $40cm/s$  (see Figure 3.23). On tests that went above this speed, clipping once again occurred (see Figure 3.24). Mr. Yokoi returned to Japan to study the situation.

## **A.6 June - September 2002: Japan**

Tokyo Sokushin developed a new model which they believed was capable of recovering broadband ground motions up to and beyond  $2m/s$ , with similar noise resolution.

## **A.7 11 - 12 November 2002: DSN — Cart Test III**

On 11-12 November 2002 Mr. Isamu Yokoi and Mr. Sotoru Wada, a engineer from Tokyo-Sokushin, visited Caltech. On 11 November, Mr Wada replaced the 3 seismometers and the feedback circuits. The new instrument was labeled the VSE-355G3. Noise tests performed in Japan indicate comparable performance from the new components to the VSE-355G2. Analysis from subsequent cart tests showed the horizontal channels could resolve motion beyond  $2m/s$ . However, a low clipping level, as before at about  $30cm/s$ , was observed on the vertical channel. Furthermore, significant cross-axis sensitivity between all components was observed during strong motion cart tests.

## **A.8 27 November 2002: DSN — Cart Test IV**

After the poor performance from the tests on 12 November, Mr Yokoi suggested rotating the sensor to see if cross-coupling would re-occur under different conditions. We re-ran the cart tests and observed similar flawed patterns to those of the 12 November tests.

## **A.9 12 March 2003: DSN — Cart Test V**

After the poor performance from the tests on 12 and 27 November, Mr Yokoi returned to Caltech. We discussed whether high frequency clipping ( $> 2g$  at  $> 200HZ$ ) was responsible for the cross-coupling. Using an oscilloscope and a hammer impulse, Mr, Yokoi demonstrated this high frequency clipping indeed gave an impulse response at about  $100s$ . It was thought that this does not adequately explain the cross-coupling as the out-of-plane and vertical components follow the velocity as observed in the in-plane motion very closely,

at a  $\sim 10s$  period.

No modification was made to the instruments. We re-ran the cart tests. Data showed some flawed patterns. Some sample data showing low vertical clipping is in Figure A.3(a) and the cross-coupling between horizontal channels in Figure A.3(b)

### **A.10 26 March 2003: DSN — Cart Test VI**

We became aware of a potential corruption of data files from 12 March test arising from an extra instrument and datalogger being attached to DSN in a laboratory in the Sub-Basement of S. Mudd. Consequently, we repeated the cart tests as in 12 March. Again, the same flaws were observed.

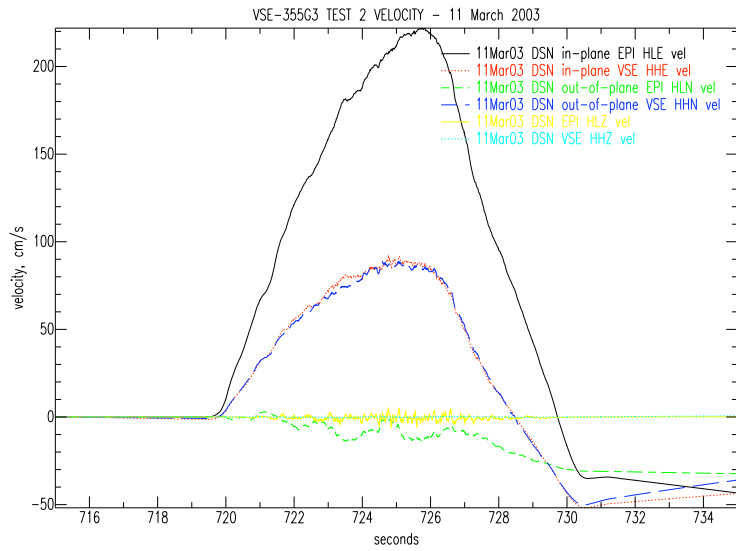
### **A.11 April - June 2003: Japan**

Tests at Sokushin revealed the Z-axis suspension spring could not linearly resist large velocity ground motions. This defect was deemed responsible for the low vertical component clip levels previously observed, as well as the cross-coupling observed between all channels. Replacement components were made for all three channels. Noise tests performed in Japan also indicate comparable performance from the new VSE-355G3 components to the old VSE-355G2. In order to observe possible low clip levels, a similar setup to the Cart Test, but in an elevator, was performed. Vertical velocities up to  $1m/s$  were observed without error, as can be seen in Figure A.4.

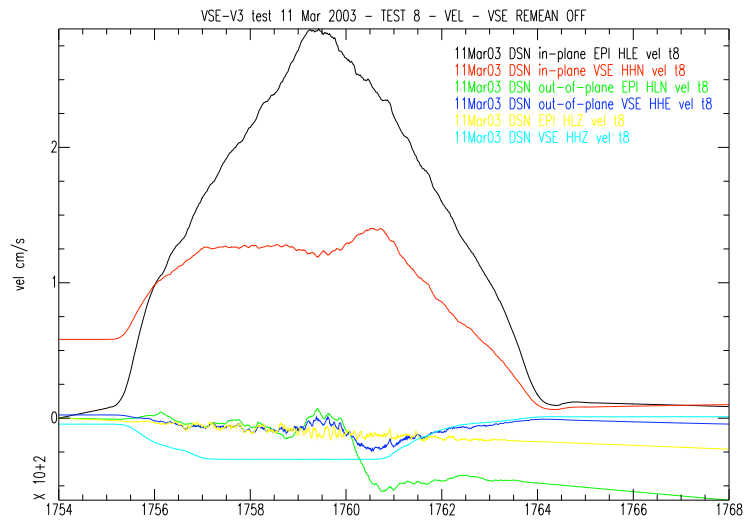
### **A.12 15 - 16 September 2003: DSN — Cart Test VI**

Mr. Soturu Wada replaced the original VSE-355G3 components with the new VSE-355G3 components for all three channels. We repeated the Cart Test, and performed a calibration test. Results from the Cart Test were very encouraging, with no low clipping observed in the horizontal channels, and no cross-talk between any channels. No large velocities were observed in the vertical direction as only a horizontal test is practical with the setup





(a) Cross-coupling



(b) Vertical clipping at 30cm/s. Also very low in-plane VSE-355G2 velocity

Figure A.3: Errors observed from cart test, 11 March 2003, for VSE-355G3.

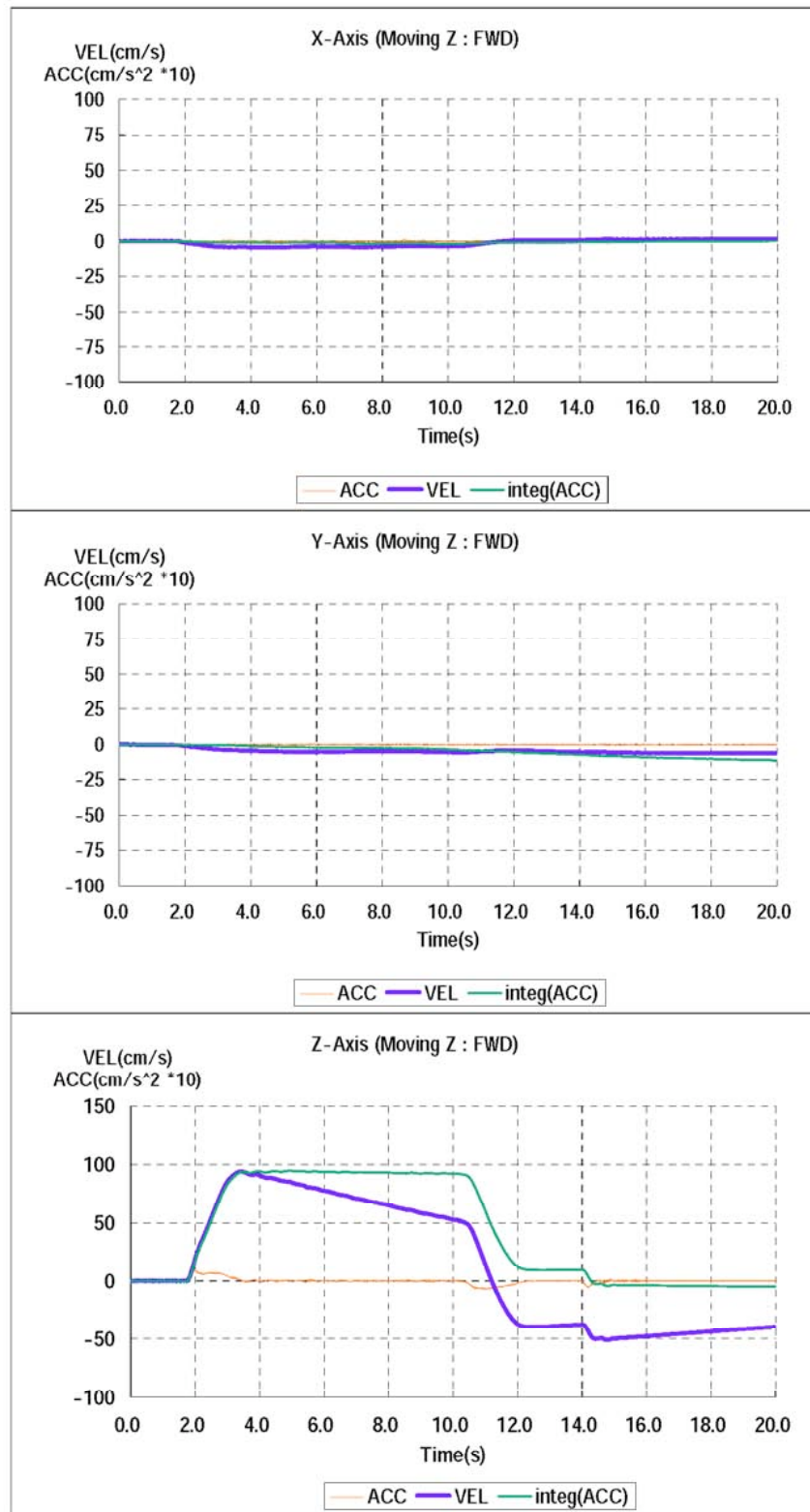


Figure A.4: Elevator test, performed in Japan by Tokyo Sokushin, June 2003, showing ability of VSE-355G3 vertical component to resolve large vertical velocities. No deconvolution of data.

at Caltech. A typical record with a large peak velocity is in Figure A.5. In this Figure, the pre-event mean is not removed, and the ‘raw’ velocity is shown to clip at  $243\text{cm/s}$ . At this stage, we became concerned with large offsets after tests, which do not return back to zero. Figure A.6 illustrates the problem. These are discussed in the next section, but basically are caused by tilting of the instrument during testing.

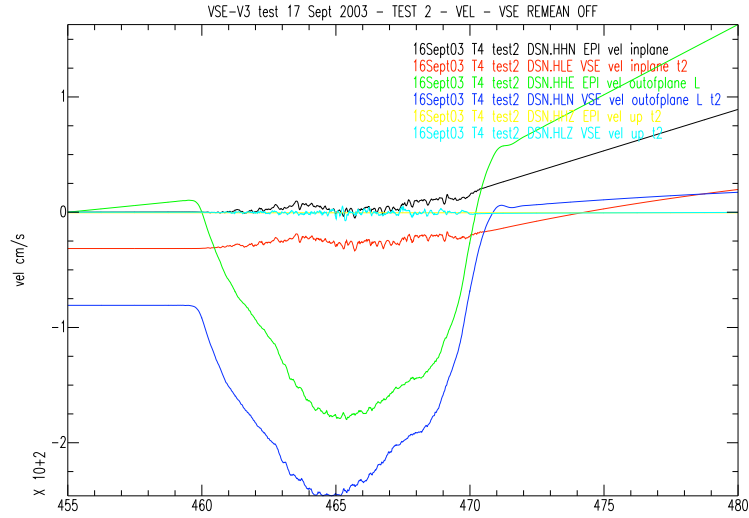


Figure A.5: Cart test, 16 September 2003 - observe VSE-355G3 clipping at  $243\text{cm/s}$ . Note all data has pre-event mean left on, and VSE-355G3 has significant offsets. In-plane/out-of-plane mix up is due to errors in channel assignments for both sensors.

The VSE-355G3 test regime shown in Figure A.6 does not include levelling in between tests and rotations, which results in large permanent velocity offsets, and so the raw output gives insight into the clipping level of the instrument. Before the cart test at  $720\text{s}$ , the E-W background velocity is at  $-166\text{cm/s}$ , indicating the instrument is severely tilted. The ensuing motions decrease the velocity further until a minimum velocity of  $-252\text{cm/s}$  is reached (which corresponds to  $-10584\text{cts}$  or  $2^{23.335}$ ,  $140\text{dB}$  of counts), whereupon the output flatlines until the motion ends. The N-S component is observed to have a similar flatline at  $-243\text{cm/s}$  during the test at  $460\text{s}$ , as seen in Figure A.5. Note this is raw sensor response, and has not been deconvolved to obtain corrected velocity response.

The clip level was not reached in tests where care is taken to level the instrument, as

the speeds upwards of  $240\text{cm/s}$  were not reached.

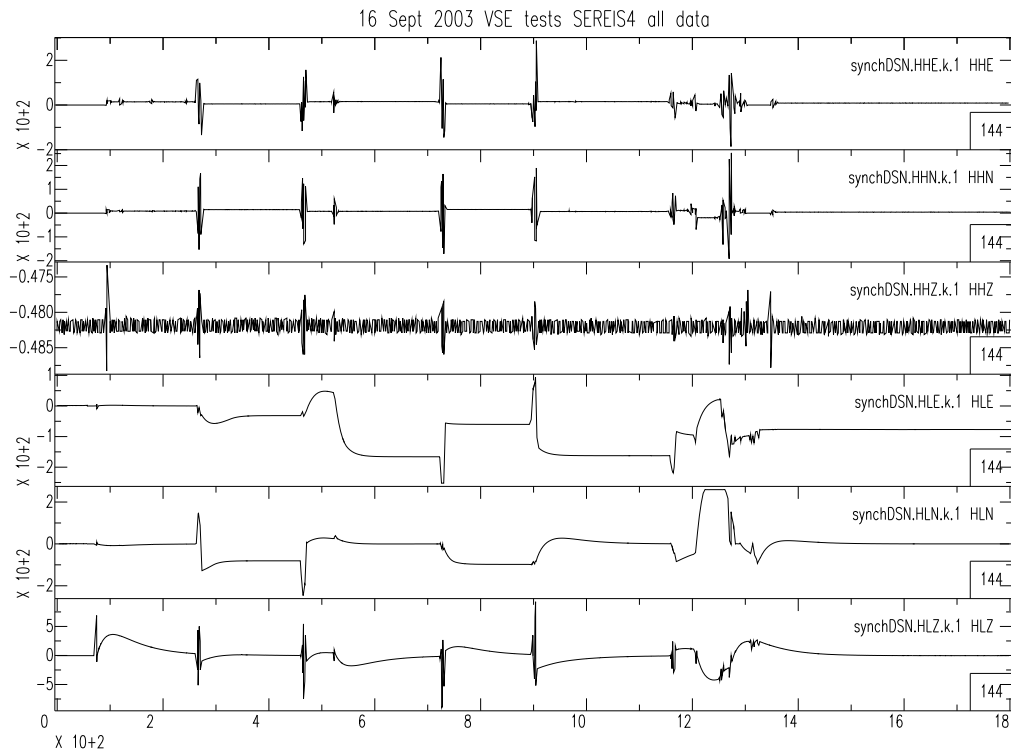


Figure A.6: Cart test — duration of a test sequence, 16 September 2003. Top 3 channels are EpiSensor acceleration ( $\text{cm/s}^2$ ), bottom 3 are the VSE-355G3 raw velocity output ( $\text{cm/s}$ ). X-axis: time in seconds. Note after tests, the VSE-355G3 sometimes exhibits static offset in output, due to tilting. Data from Figure A.5 is from the test occurring between 400 and 500s. Spikes at 80s are due to turning power on. Forward test at 270s, backward at 470s. VSE rotated  $90^\circ$  anti-clockwise at 515s, with 2 more tests following. Transients after 1150s are of unknown origin, possibly from changing pin connections or modifying the power source. VSE-355G3 E-W channel is observed to clip during the test occurring at 720s, at  $-252\text{cm/s}$ . At 470s, the N-S channels clips at  $-243\text{cm/s}$ .

Results from the calibration test are in Figure A.7. A problem was also identified in this test, with behaviour not commensurate with a velocity meter observed in the 2 horizontal channels. This test was performed under the instruction of the manufacturer. A signal generator applied a step function in current, with a period of  $5\text{mins}$ . A capacitor was placed in the circuit between the signal generator and the calibration coil, which had the effect of

differentiating the input signal to the calibration coil, so the current applied to calibration coil was in the form of an impulse, or  $\delta$ -function. Thus the input to each channel was an impulse in acceleration. The expected output should be as in Equation 3.20 and as seen Figure 3.5. For each of the three components, the best fit model was determined, varying  $t_0, H(t - t_0), \omega_0$  and  $\beta$ , for the observed VSE output. Also included is the expected model to the integrand and double integrand of the output, as given in Eqns. 3.19 and 3.21. Figure A.7 provides a graphical comparison for the best fit and observed VSE data for such an acceleration impulse input. The vertical channel can be well modelled as an SDOF, but the EW and NS deviate from this idealised behaviour.

In summary the best fit SDOF solution is  $T_0 = 110s, \zeta = 0.64$  E-W component,  $T_0 = 107s, \zeta = 0.60$  N-S, and  $T_0 = 105.8s, \zeta = 0.64$  Vertical. These free periods are significantly longer than those of the VSE-355G2. The variation in these solutions were larger than expected, and the horizontal channels cannot be approximated by this SDOF solution.

### **A.13 October - November 2003: CRP**

Ambient noise tests and simple calibration tests using only the levelling screws were performed with the instrument deployed alongside an STS-2 and a CMG-1T at the Robinson Pit CISM station CRP. The system was observed to behave well during the small M3.6 Simi Valley earthquake  $55km$  from the site, and during ambient noise analysis (see Figure 5.8). Unfortunately, the screw test, shown in Figure A.8 revealed very strange instrument response to a simple step in acceleration, with permanent offsets in the E-W component, and a response longer in period than that from a  $100s$  SDOF.

CRP was logged using a Q680, CRPA with a Q330. As CRPA, and to some extent CRP, are test sites, sensors and dataloggers are interchanged quite frequently.

### **A.14 24 - 26 November 2003: CRP and DSN**

Mr. Yokoi visited Caltech again, to investigate the cross-coupling problems, and faulty output from calibration tests. On 24 November 2003, after reviewing and modifying the

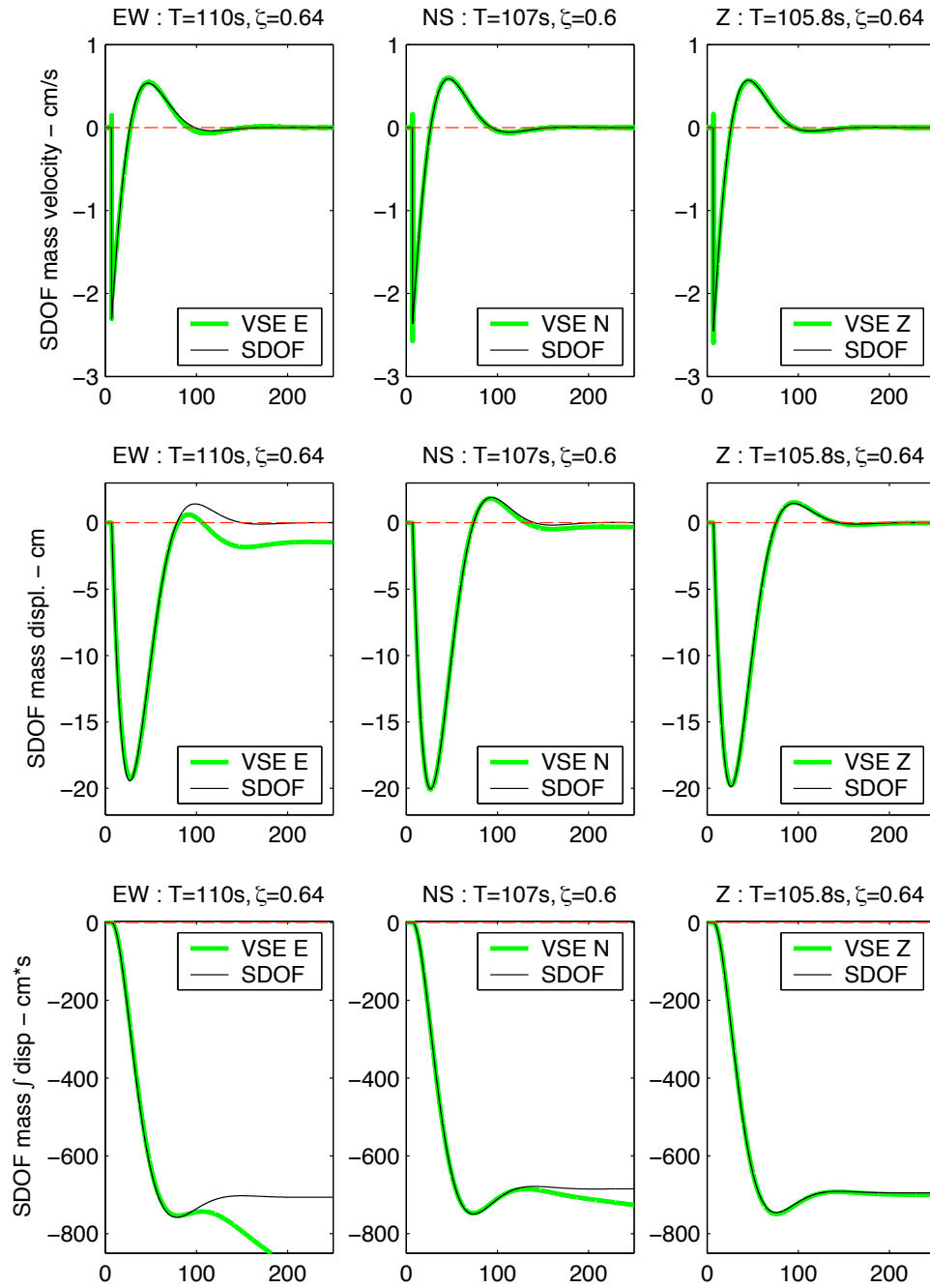


Figure A.7: Calibration coil response test, VSE-355G3, September 2003

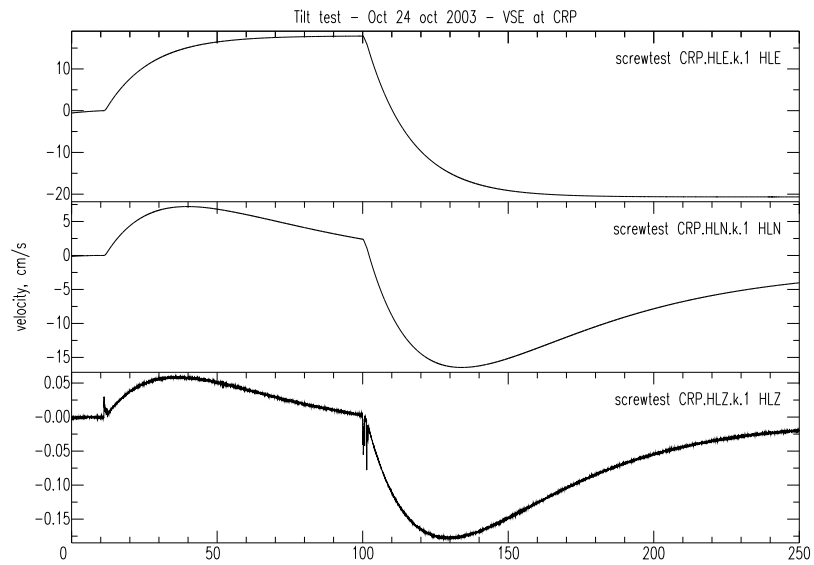


Figure A.8: Tilt test using levelling screws in normal operation, October 2003, VSE-355G3 model. Contrast with VSE-355G2 performance in March 2002 (Figure A.2). Screw turned anti-clockwise 1/4 turn at 10s, then 1/2 turn clockwise at 100s. Note:  $\sim 100s$  SDOF should return to zero offset after  $\sim 100s$ , as in Figure 3.6. E-W component has permanent offset; all 3 components take  $> 100s$  for the transient to settle.

pin connections, data was collected from tilt tests, and simple battery input tests to the calibration coils. Figure A.9 shows results from the screw test, which shows good operation, very similar to the expected result seen in Figure 3.6. All three components have a corner at approximately 105s, with more variability in the damping, ranging from 0.555 to 0.64. Figure A.10 shows results from the battery test, where the connections to the input for the calibration coil are ‘touched’ briefly to a standard AA battery, which simulates a  $\delta$ -function input. All output is compared to the models determined in Figure A.9. The N-S and Vertical performance is very similar, but the E-W channel output is very different from that expected. This prompted a complete review of the pin connections. Once this was complete, the battery test indicated good compatibility with the tilt test results for all three components.

As the calibration tests were satisfactory, the instrument was moved back to South Mudd and the Cart Test was run again on 25 November 2003. In the morning a suite of tests were run, and though the clip level was observed to be above  $2m/s$ , and cross-coupling was not observed, it was noted that after certain runs, and after an instrument rotation (done to identify any cross coupling, and check if each horizontal channel was capable of reaching the large velocities), there were large static offsets in the velocity timeseries. It was determined this was due to tilting of the instrument. In the afternoon, tests were performed with care taken to re-level the instrument if the bubble had been observed to move. Figure A.11 plots the timeseries for the afternoon tests, and includes the E-W component of the FBA-23, and all three components of the VSE-355G3. It was noted that the bubble level did indeed move around, especially after a rotation. Once this was corrected, the baseline velocity re-zeroed. A self levelling device in the instrument saturates when tilts become too large, meaning the instrument cannot re-center. This can be monitored externally, as the tilt channels may not re-center if voltages required to re-center rise above 12V. If the tilt voltage reaches this level, it will remain high, if this level is not reached, the tilt voltage will return to zero. It is unlikely this channel will be monitored remotely. However, in the field, this can be observed from static offsets in the baseline velocity output. The instrument needs to be manually re-levelled to remove the effect. It is not known whether the magnitude of tilt required to create this problem are larger than that expected even in



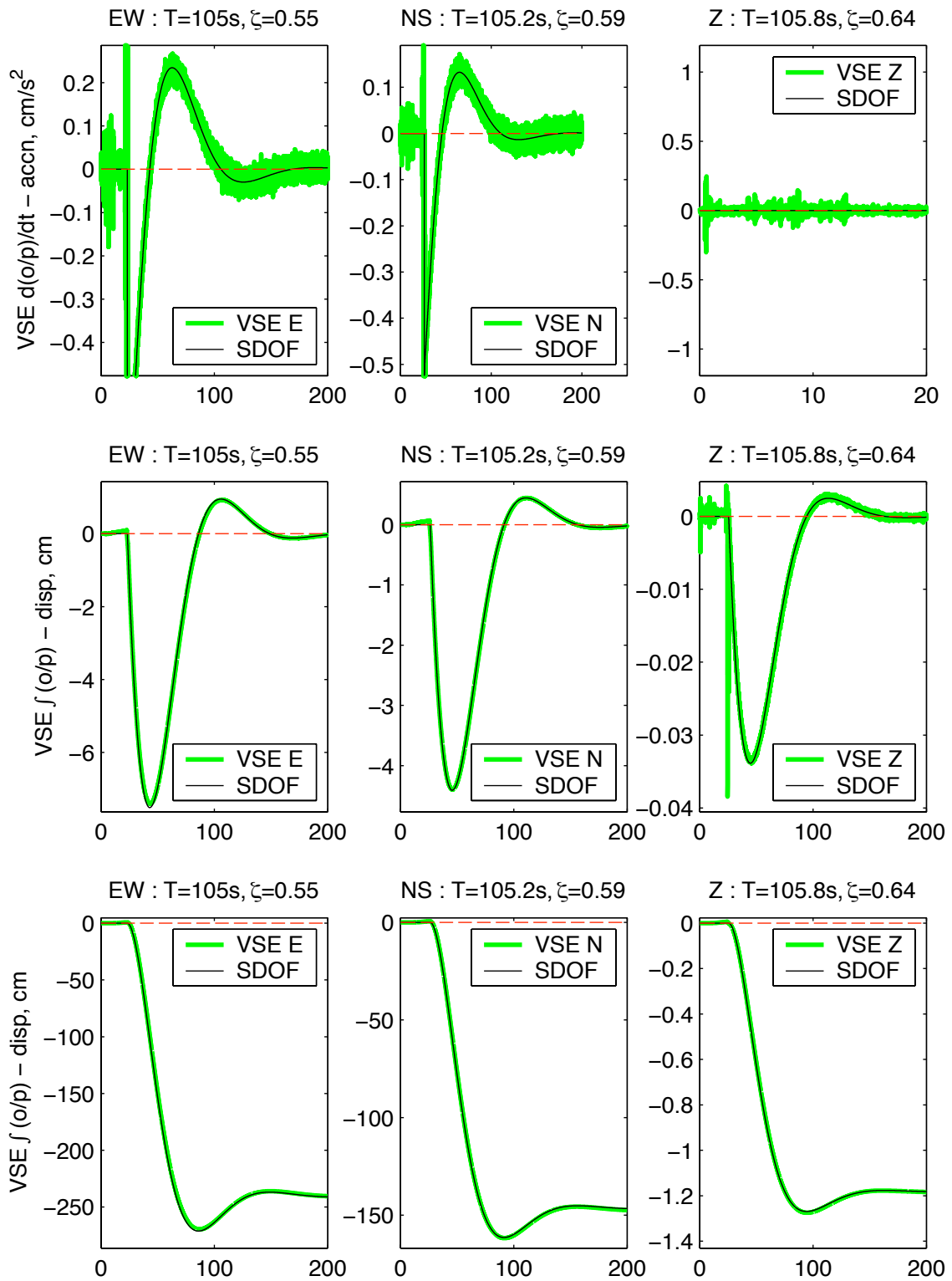


Figure A.9: Tilt test using levelling screws in normal operation, 24 November 2003, VSE-355G3 model. Good performance.

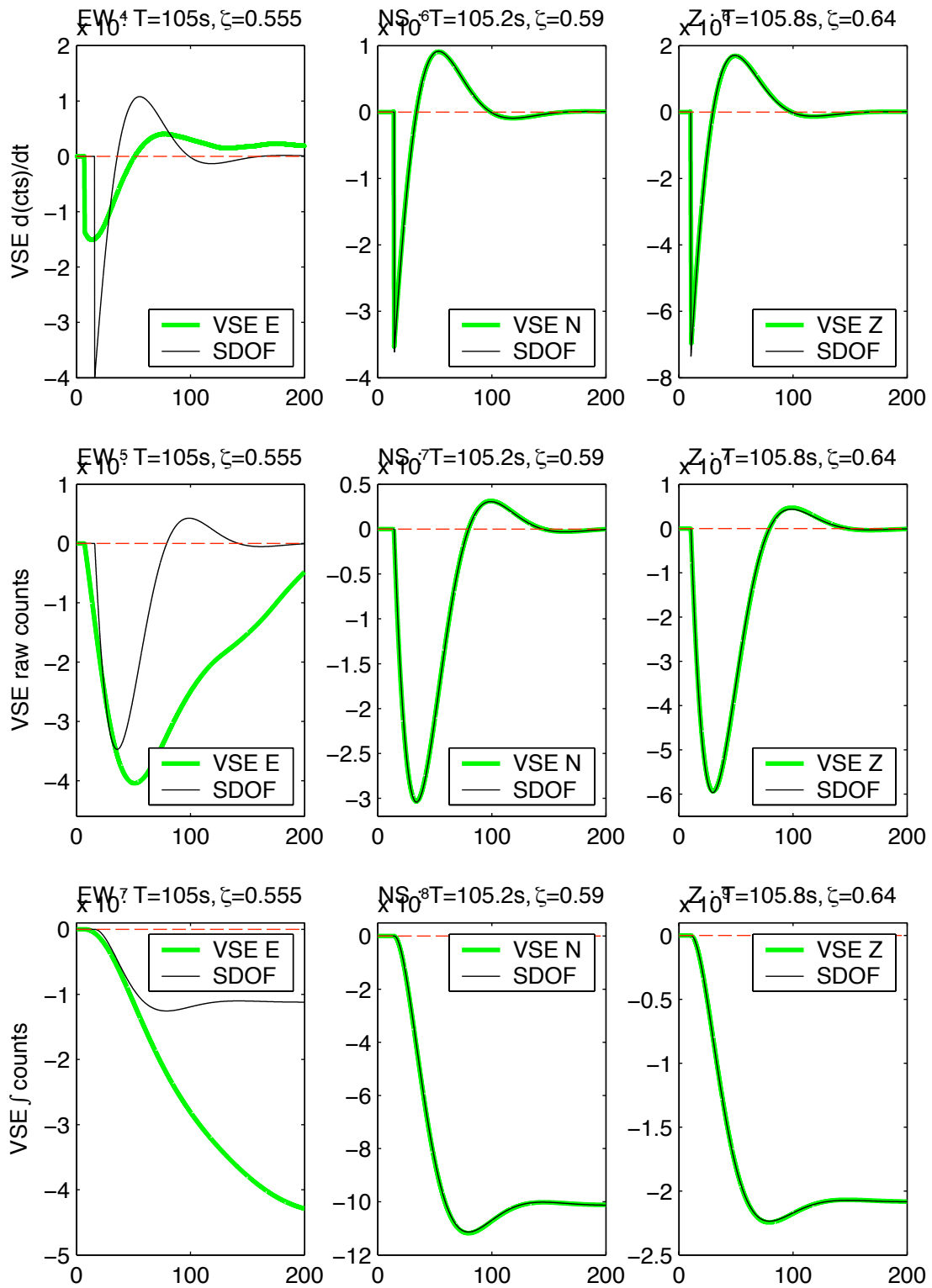


Figure A.10: Battery test using calibration coil input, 24 November 2003, VSE-355G3 model. Poor performance from E-W channel.

severe ground motions. No further research was taken into investigating exactly what tilt magnitude causes the problem. We do note that some large records recorded on Tokyo-Sokushin strong motion velocity instruments during the Tokachi-Oki earthquake do have unexplained offsets in the deconvolved velocity output, which could be due to this effect. This is a clear disadvantage of this instrument compared to an FBA, which can continue to operate with large tilt,

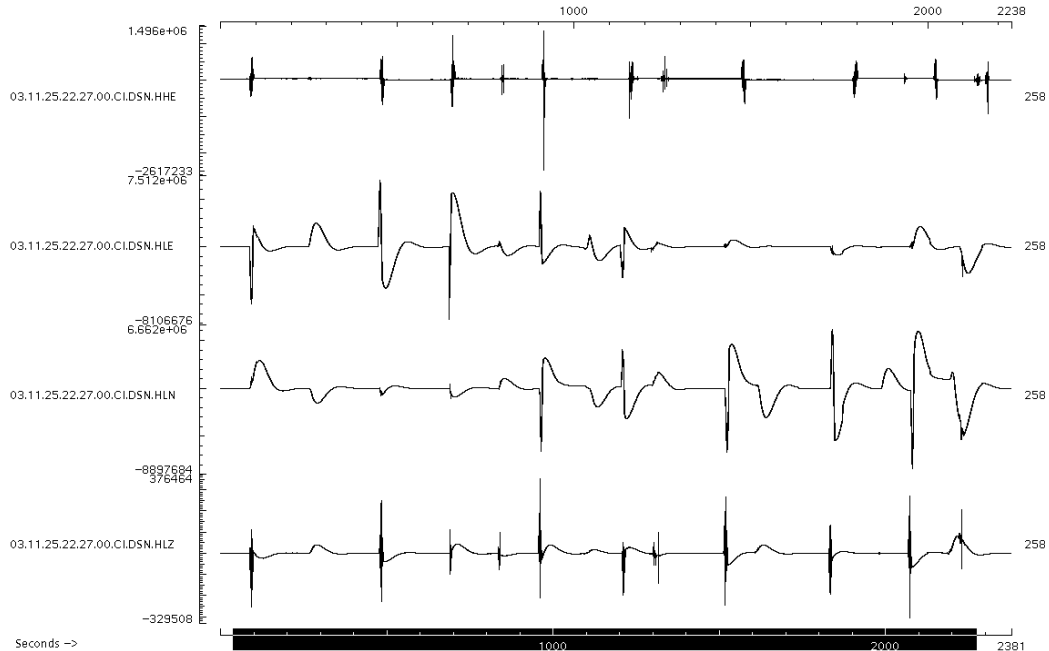


Figure A.11: Cart Test — duration of test sequence, 25 November 2003, with re-levelling after every run. Top channel is E-W EpiSensor acceleration, bottom 3 are the VSE-355G3 raw velocity output. Y-axis is counts. Note after tests, the VSE-355G3 sometimes exhibits static offset in output, due to tilting, which is corrected by re-levelling the instrument. Compare to Figure A.6, without levelling. Forward test at 90s, re-levelling at 270s, backward at 480s, forward at 700s. The instrument was rotated  $45^\circ$  and re-levelled at 830s. A backward test at 960s, re-levelled at 1100s, and forward at 1200s. Another  $45^\circ$  rotation at 1300s, backward at 1500s, re-levelled at 1600s. Forward at 1830s, re-levelled at 2000s. Forward at 2080s, backward at 2200s.

## A.15 23 January 2004: CRP and DSN

After a few months of continuous recording at CRP, another tilt test was performed. Results are in Figure 5.4 and Figure A.12. The equivalent SDOF for the N-S and Z VSE-355G3

channels are identical to the observations from the same test in November 2003, Figure A.9; the E-W component has the same damping, but there is a small increase in free period from 105.0s to 105.5s.

The STS-2 at CRP was removed for use elsewhere in the CISN in late October 2003. This was before the pin connection problems had been resolved. A CMG-1T was the broadband high-gain sensor replacement. Noise and earthquake data (from the San Simeon earthquake, 24 December 2003), have been recorded, and are analysed in Chapter 5. Dynamic range performance was found to be similar to that of the VSE-355G2, with the instrument capable of about 132*dB* of signal.

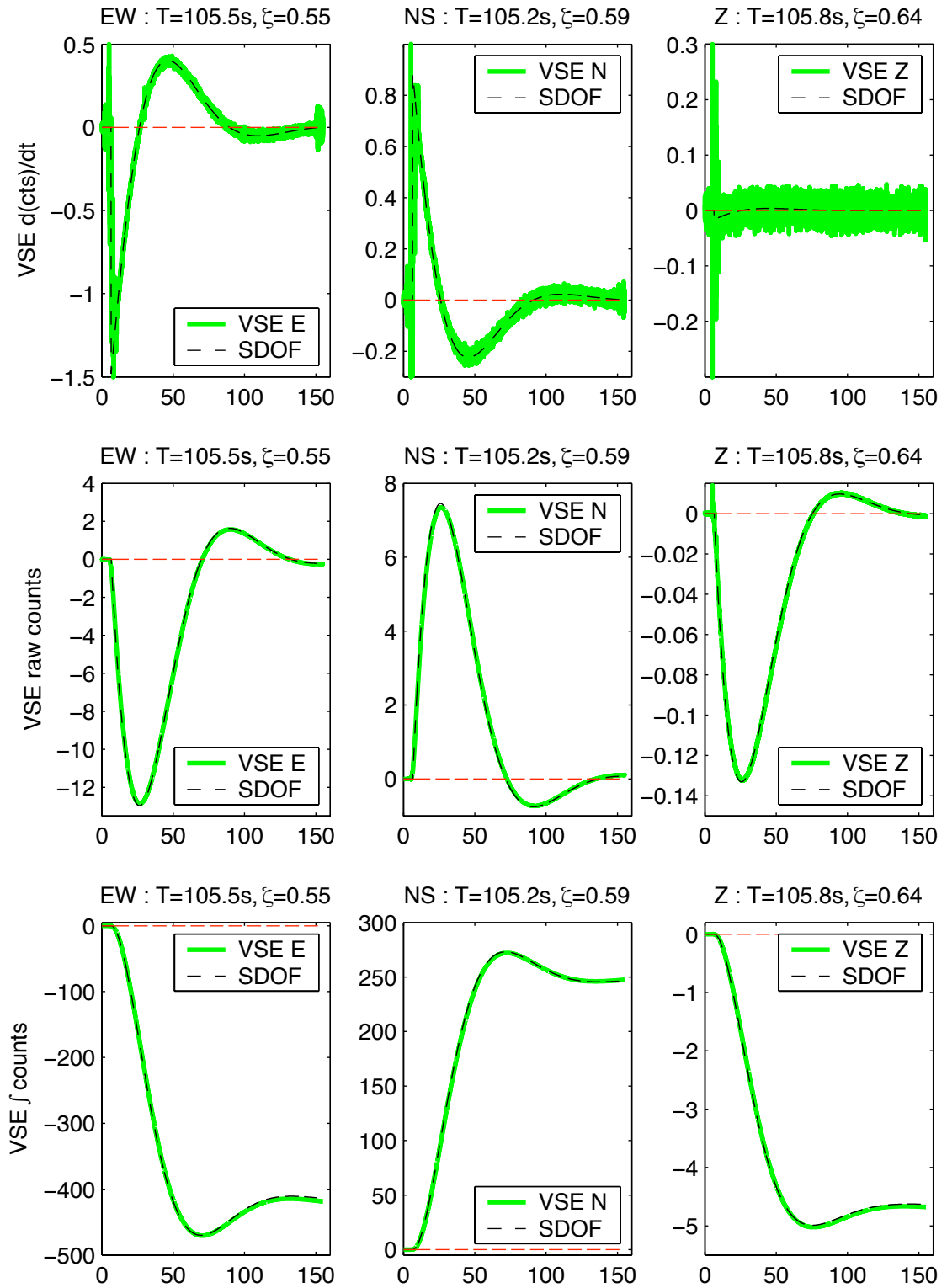


Figure A.12: Response to a tilt, caused by adjusting the levelling screw, January 2004

## Appendix B Previous Studies of Millikan Library

Since the completion of the Library in 1966, Millikan has survived (and recorded) numerous moderate earthquakes within and nearby the greater Los Angeles area. Most notable among these are the Borrego Mountain ( $M6.5, \Delta = 213km$ ), Lytle Creek ( $M5.3, \Delta = 56km$ ), San Fernando ( $M6.6, \Delta = 39km$ ), Whittier Narrows ( $M5.9, \Delta = 10km$ ), Pasadena ( $M5.0, \Delta = 0km$ ), Sierra Madre ( $M5.6, \Delta = 20km$ ), Landers ( $M7.3, \Delta = 187km$ ), Big Bear ( $M6.5, \Delta = 145km$ ), Northridge ( $M6.7, \Delta = 47km$ ), and Hector Mine ( $M7.1, \Delta = 210km$ ).

In the decade following its construction, numerous published reports investigated the complex dynamic properties of the structure, with the likely conclusion that the fundamental periods are strongly influenced by soil-structure interaction, and a significant proportion of modal motion is due to rocking and sliding (Luco et al, 1986). It was observed that the building also softened permanently after the strong shaking encountered in the M6.6 1971 San Fernando earthquake.

A complete summary of the various studies into the frequency characteristics of the building may be found in Tables B.1 and B.2. These include both forced and ambient testing of the structure, and indicate an evolution in the frequency and damping of the structure, most notable affected by the M6.7 San Fernando event which occurred on 9 February 1971 and resulted in the permanent lengthening of the free periods and increased damping for the structure. A permanent shaker installed on the roof allowed forced vibrations at frequencies up to about 10Hz. Table B.3 contains the references used to compile Tables B.1 and B.2. Most years, forced vibration tests are carried out on the building in Caltech Civil Engineering Class 180 — Experimental Methods in Civil Engineering. Each spring the fundamental modeshapes and natural frequencies are recorded. This provides a ‘data point’ for each year. An attempt was made to gather as many of these un-published results as possible.

Figure B.1 presents a summary plot of the tables. It is similar to Figure 6.4, but contains the extra information included in these tables.

Shortly after construction was completed, a PhD study by Kuroiwa (1967) suggested the building behaved non-linearly as a ‘softening system’, since the natural frequencies reduced as the applied excitation increased. The observed effect was small, with the N-S mode reduced 2.9% as force increased by 3.8, the E-W mode reduced 2.7% as force increased by 7.5, and the torsional mode reduced 1.2% as force increased by 2.1. Damping values also appear to be non-linear, they are observed to increase with increased excitation.

It was also noted that the building is very stiff for its height, but may be readily explained by the very rigid structural system for a building of this height.

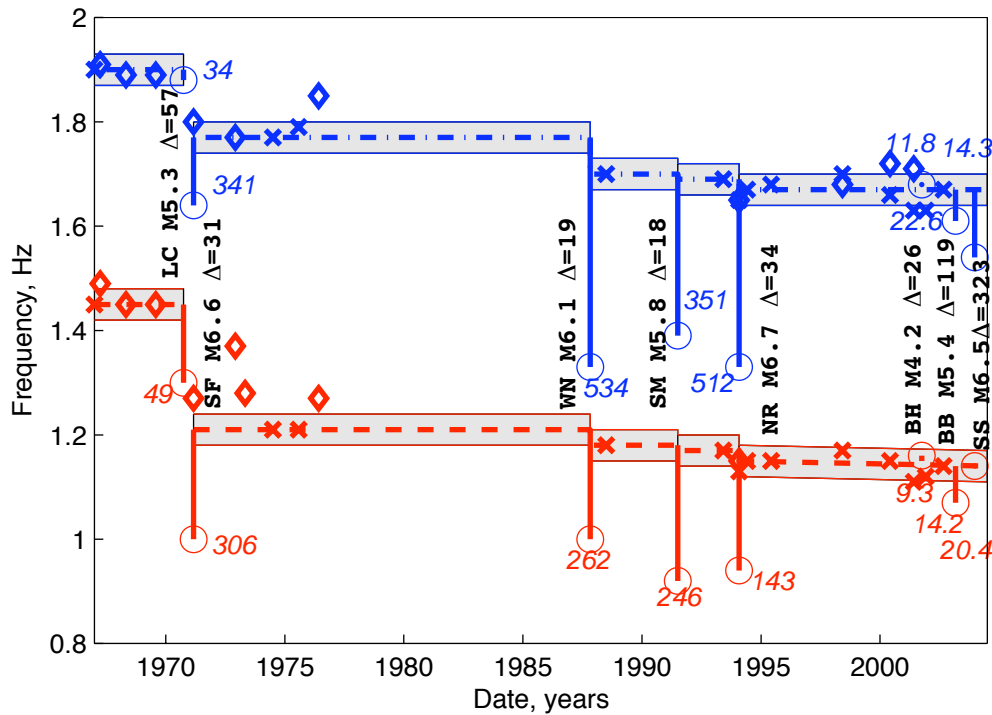


Figure B.1: Graphical interpretation of Tables B.1 and B.2. Dashed lines are E-W natural frequencies, dashed-dotted are N-S natural frequencies, all from forced vibration testing. Shaded area is the likely region of natural frequencies taking into consideration errors in measurement, due to unknown shaker weight configuration and weather conditions for each test, and experimental error. Crosses and diamonds indicate the actual time and frequency of a forced vibration and ambient measurement respectively. Circles indicate natural frequency estimated from the strong motion record of the event, with the number in italics giving the peak acceleration recorded for the event ( $cm/s^2$ ).

Test	East - West		North - South		Torsional		Remark
	$f_0$ [ $\zeta_0$ ]	$f_1$ [ $\zeta_1$ ]	$f_0$ [ $\zeta_0$ ]	$f_1$ [ $\zeta_1$ ]	$f_0$ [ $\zeta_0$ ]	$f_1$ [ $\zeta_1$ ]	
1966-1967 <sup>1</sup>	1.46-1.51 [0.7-1.7]	6.2	1.89-1.98 [1.2-1.8]	-	2.84-2.90 [0.9-1.6]	-	A,F,M
Mar 1967 <sup>2</sup>	1.49 [1.5]	6.1	1.91 [1.6]	-	2.88	-	A
Apr 1968 <sup>3</sup>	1.45	6.1	1.89	9.18	2.87	9.62	A
Jul 1969 <sup>4</sup>	1.45	5.90	1.89	9.10	-	-	A
Sep 12 1970 <sup>5</sup>	1.30-1.50	-	1.90-2.10	-	-	-	E (LC)
Sep 12 1970 <sup>6</sup>	1.30	-	1.88	-	-	-	E (LC)
~ M6.7 February 9 1971 San Fernando Earthquake (SF) @ 44km ~							
Feb 9 1971 <sup>5</sup>	1.00-1.50	-	1.50-1.90	-	-	-	E (SF)
Feb 9 1971 <sup>7</sup>	0.82-1.43 [1.0-13.0]	-	-	-	-	-	E (SF)
Feb 9 1971 <sup>8</sup>	1.02-1.11 [3.5-5.5]	-	-	-	-	-	E (SF)
Feb 9 1971 <sup>9</sup>	1.03 [0.07]	4.98 [0.06]	1.61 [0.06]	7.81 [0.06]	-	-	E (SF)
Feb 9 1971 <sup>10</sup>	1.02 [0.06]	4.93 [0.05]	1.61 [0.06]	7.82 [0.05]	-	-	E (SF)
Feb 9 1971 <sup>6</sup>	1.00	-	1.64	-	-	-	E (SF)
Feb 1971 <sup>11</sup>	1.27 [2.5]	5.35 [0.9]	1.8 [3]	9.02 [0.2]	2.65 [2]	9.65 [0.5]	A
Feb 1971 <sup>4</sup>	1.30	-	-	-	-	-	A
Dec 1972 <sup>4</sup>	1.37	-	1.77	-	-	-	M
Apr 1973 <sup>12</sup>	1.28 [1.3]	-	-	-	-	-	A
1974 <sup>13</sup>	1.21	-	1.76	-	-	-	F
Jul 1975 <sup>14</sup>	1.21 [1.8]	-	1.79 [1.8]	-	-	-	F
May 1976 <sup>9</sup>	1.27	-	1.85	-	2.65	-	A
~ M6.1 October 1 1987 Whittier Narrows Earthquake (WN) @ 19km ~							
Oct 1 1987 <sup>10</sup>	0.932 [0.04]	4.17 [0.08]	1.30 [0.06]	6.64 [0.18]	-	-	E (WN)
Oct 1 1987 <sup>6</sup>	1.00	-	1.33	-	-	-	E (WN)
Oct 4 1987 <sup>10</sup>	0.98	-	1.43	-	-	-	E(WN M5.3)
Oct 16 1987 <sup>10</sup>	1.20	-	1.69	-	-	-	E(WN M2.8)
May 1988 <sup>11</sup>	1.18	-	1.70	-	-	-	F
~ M5.8 June 28 1991 Sierra Madre Earthquake (SM) @ 18km ~							
June 28 1991 <sup>6</sup>	0.92	-	1.39	-	-	-	E (SM)
May 1993 <sup>15</sup>	1.17	-	1.69	-	2.44	-	F
~ M6.7 January 17 1994 Northridge Earthquake (N) @ 34km ~							
Jan 17 1994 <sup>6</sup>	0.94	-	1.33	-	-	-	E (N)
Aug 2002 <sup>18</sup>	1.14 [2.28]	4.93	1.67 [2.39]	7.22	2.38 [1.43]	6.57	F

Table B.1: Summary of Millikan Library modal frequency and damping analysis experiments, 1967-1994.  $f_0$  and  $f_1$  are the fundamental frequency and the first overtone, in Hz.  $\zeta_0$  and  $\zeta_1$  are the corresponding damping ratios, in %. References are found in Table B.3. A: Ambient, M: Man Excited, F: Forced Vibration, E: Earthquake motions [LC: Lytle Creek]



Test	East - West		North - South		Torsional		Remark
	$f_0$ [ $\zeta_0$ ]	$f_1$ [ $\zeta_1$ ]	$f_0$ [ $\zeta_0$ ]	$f_1$ [ $\zeta_1$ ]	$f_0$ [ $\zeta_0$ ]	$f_1$ [ $\zeta_1$ ]	
1966-1967 <sup>1</sup>	1.46-1.51 [0.7-1.7]	6.2	1.89-1.98 [1.2-1.8]	-	2.84-2.90 [0.9-1.6]	-	A,F,M
Mar 1967 <sup>2</sup>	1.49 [1.5]	6.1	1.91 [1.6]	-	2.88	-	A
~ M6.7 February 9 1971 San Fernando Earthquake (SF) @ 44km ~							
Feb 9 1971 <sup>6</sup>	1.00	-	1.64	-	-	-	E (SF)
May 1976 <sup>9</sup>	1.27	-	1.85	-	2.65	-	A
~ M6.1 October 1 1987 Whittier Narrows Earthquake (WN) @ 19km ~							
Oct 1 1987 <sup>10</sup>	0.932 [0.04]	4.17 [0.08]	1.30 [0.06]	6.64 [0.18]	-	-	E (WN)
Oct 1 1987 <sup>6</sup>	1.00	-	1.33	-	-	-	E (WN)
Oct 4 1987 <sup>10</sup>	0.98	-	1.43	-	-	-	E(WN M5.3)
Oct 16 1987 <sup>10</sup>	1.20	-	1.69	-	-	-	E(WN M2.8)
May 1988 <sup>11</sup>	1.18	-	1.70	-	-	-	F
~ M5.8 June 28 1991 Sierra Madre Earthquake (SM) @ 18km ~							
June 28 1991 <sup>6</sup>	0.92	-	1.39	-	-	-	E (SM)
May 1993 <sup>15</sup>	1.17	-	1.69	-	2.44	-	F
~ M6.7 January 17 1994 Northridge Earthquake (N) @ 34km ~							
Jan 17 1994 <sup>6</sup>	0.94	-	1.33	-	-	-	E (N)
Jan 19 1994 <sup>15</sup>	1.13	-	1.65	-	2.39	-	F
Jan 20 1994 <sup>15</sup>	1.13	4.40-4.90	1.65	8.22-8.24	2.39	-	A
	[1.2-2.1]	[1.0]	[0.7-1.5]	[0.2-0.3]	[0.3-0.5]		F
May 1994 <sup>16</sup>	1.15 [1.38]	-	1.67 [1.46]	-	2.4 [1.18]	-	F
May 1995 <sup>16</sup>	1.15 [1.44]	-	1.68 [1.25]	-	2.42 [1.15]	-	F
May 1998 <sup>16</sup>	1.17 [1.4]	-	1.70 [1.3]	-	2.46	-	F
May 1998 <sup>16</sup>	-	-	1.68	1.5	-	-	M
May 2000 <sup>16</sup>	1.15 [3]	-	1.66 [3]	-	2.41 [2.5]	-	F
May 2000 <sup>16</sup>	-	-	1.72 [0.8]	-	-	-	A
May 2001 <sup>16</sup>	1.11 [3.25]	-	1.63 [3.69]	-	2.31 [2.9]	-	F
May 2001 <sup>16</sup>	-	-	1.71 [1.2]	-	-	-	M
Dec 2001 <sup>17</sup>	1.12 [1.63]	-	1.63 [1.65]	-	2.34	-	F
Sep 9 2001 <sup>6</sup>	1.16	-	1.68	-	-	-	E (BH M4.2)
Aug 2002 <sup>18</sup>	1.14 [2.28]	4.93	1.67 [2.39]	7.22	2.38 [1.43]	6.57	F
Feb 22 2003 <sup>6</sup>	1.07	-	1.61	-	-	-	E (BB M5.4)

Table B.2: Summary of Millikan Library modal frequency and damping analysis experiments, 1987-2003.  $f_0$  and  $f_1$  are the fundamental frequency and the first overtone, in Hz.  $\zeta_0$  and  $\zeta_1$  are the corresponding damping ratios, in %. References are found in Table B.3. A: Ambient, M: Man Excited, F: Forced Vibration, E: Earthquake motions [BH: Beverly Hills, BB: Big Bear]

<b>Footnote #</b>	<b>Reference</b>	<b>Remarks</b>
1	Kuroiwa (1967)	<i>forced, ambient, man excitations</i> – <i>during and immediately after construction, Library not full</i>
2	Blandford et al. (1968)	<i>ambient</i>
3	Jennings and Kuroiwa (1968)	<i>ambient</i>
4	Udwadia and Trifunac (1973)	<i>ambient</i>
5	Udwadia and Trifunac (1974)	<i>Lytle Creek, San Fernando</i> – <i>based on transfer functions</i>
6	Clinton et al. (2004), this Thesis	<i>Earthquakes</i> – <i>estimated from strong motion records</i>
7	Iemura and Jennings (1973)	<i>San Fernando</i>
8	Udwadia and Marmarelis (1976)	<i>San Fernando</i> – <i>based on linear model</i>
9	McVerry (1980)	<i>SanFernando; ambient</i>
10	Beck and Chan (1995)	<i>SanFernando, Whittier MODEID</i>
11	Teledyne-Geotech-West (1972)	<i>ambient - 1mth after San Fernando</i> – <i>Also Vertical <math>f_0 = 3 - 4\text{Hz}</math>, high <math>\zeta</math>.</i>
12	Udwadia and Marmarelis (1976)	<i>San Fernando</i>
13	Foutch et al. (1975)	<i>forced</i>
14	Luco et al. (1987)	<i>forced</i>
15	Beck et al. (1994)	<i>forced, ambient</i> – <i>Also Jan 20 Ambient test: EW3 at 7.83Hz</i>
16	CE180 Caltech - various students	<i>forced</i>
17	Favela, personal communication	<i>forced</i>
18	Bradford et al. (2004)	<i>forced</i> – <i>Also EW3 at 7.83Hz</i>

Table B.3: References which correspond to footnote numbers in Tables B.1 and B.2

What is more unusual is the ratio of fundamental mode to first overtone for each direction, which, using the recent results of Favela (personal communication, 2002) are  $\sim 6.6$  for the E-W and  $\sim 5.6$  for the N-S direction. From simple theory on beams in pure bending and shear (Iwan, 1998), we expect a ratio of approximately 3 for buildings responding predominantly in shear, and 6.3 for buildings responding predominantly in bending. From the actual values observed in the building, which we expect to respond as a shear building, we must conclude there is a more complicated explanation for the dynamic response of the Library than the simple beam theory allows. This is most likely due to a soil-structure interaction often suggested in the literature, but never fully explained or quantified.

Numerous studies (Kuroiwa, 1967; Foutch, 1976) find a significant portion of roof motion may be accounted for from rocking and translation observed in the basement. Studies after the 1971 San Fernando earthquake find up to 30% of the N-S building motion at resonance may be attributable to foundation compliance (Foutch, 1976), with basement translation increasing by a factor of 2 and basement rotation by a factor of 25 more after the earthquake. (Foutch and Jennings, 1978) suggest the increased foundation compliance may be due to brittle failure of retaining walls, sidewalks and concrete slabs at the ground floor. They include evidence of compressional spalling and cracking of concrete at the ground level.

Udwadia and Trifunac (1974) employ a moving window analysis of the time-series recorded at Millikan for the 1971 San Fernando event and observe marked reductions in the resonant frequencies in both the N-S and E-W directions within the duration of strong shaking.

## Appendix C Millikan Library Dynamic Response to Forced Vibration

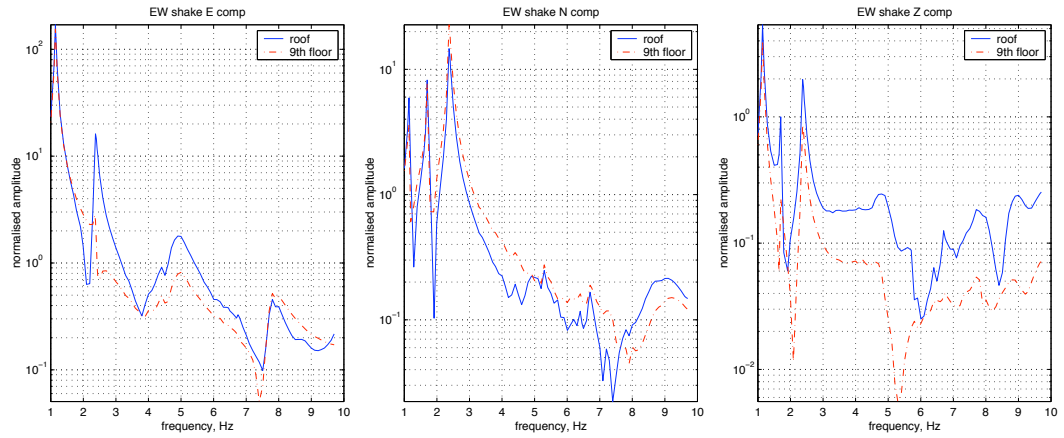
During the Summer of 2002, a suite of investigations into the dynamic response of Millikan Library were performed by myself, Samuel Case Bradford and Javier Favela. An EERL report (Bradford et al, 2004) documents this in detail, but I summarise the important findings here.

In June 2002, we performed a frequency sweep of the building, from below the natural frequencies at  $1Hz$  to  $9.7Hz$ , the upper bound frequency limit of the shaker. Data was recorded on the SCSN Station MIK, and a portable Ranger seismometer placed on the roof. From this sweep, we were able to determine the natural frequencies of the building, and the damping ratios.

The building was shaken in both the E-W and N-S directions. Frequency amplitude plots with force normalisation (different weight configurations were used for different frequencies to maximise building displacement) are presented for both directions in Figures C.1 and C.2.

From these plots we identified the natural frequencies for use in a modal evaluation of the building. For this experiment, we had Arnie Acosta, of USGS, with us to trigger the 36 channel USGS array, which has at least 3 channels per floor (1 E-W, 2 N-S, to determine torsion). On 28 August 2002, we shook the building again near these frequencies with frequency increases of about  $0.03Hz$ , the resolution of the shaker controller. We also shook using differing weight configurations to see if the weight had an effect on the natural frequency.

The results of this experiment is summarised in the Table C.1. The weight configurations vary from full weights,  $\sim 1/2$  weights, and no weights in the shaker. More weight in the shaker, which corresponds to a larger shaking force applied to the building, results in slightly decreased natural frequencies (the building appears ‘softer’). From this table, we

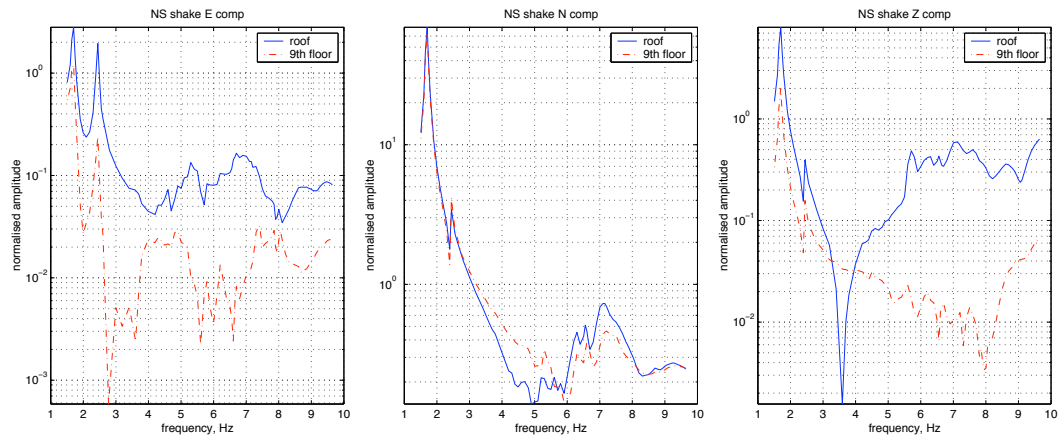


(a) E component

(b) N component

(c) Z component

Figure C.1: Millikan Library frequency sweep - E-W shake



(a) E component

(b) N component

(c) Z component

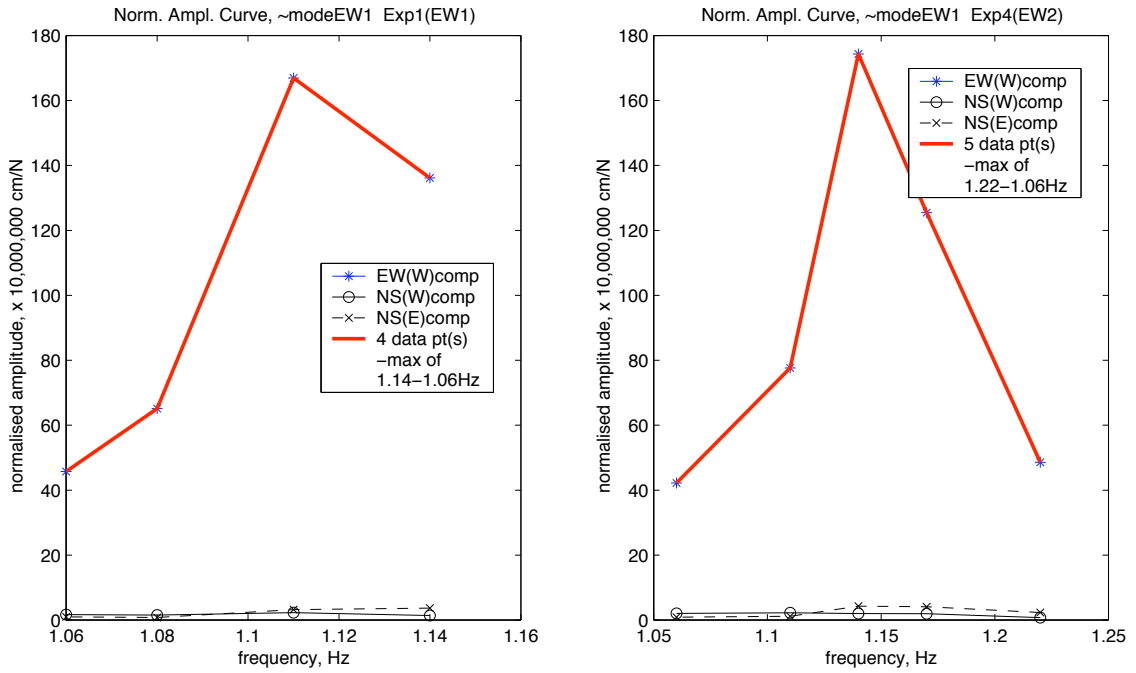
Figure C.2: Millikan Library frequency sweep - N-S shake

also see dramatic differences in the amount of soil-structure interaction for the different modes. In this experiment, the interaction is identified by taking the ratio of displacement at the roof which is due to rocking and translation of the basement, to the total roof displacement. Basement rocking is determined using the 3 vertical channels at the basement, and basement displacement from the 3 horizontal basement channels. All 3 identified E-W modes have very little soil-structure interaction ( $< 3\%$ ), and both N-S modes have significant (Fundamental N-S has 30%, first overtone has 21%) soil-structure interaction. For the torsional modes, this soil-structure interaction is defined as proportion of roof rotation due to basement rotation - this ratio is negligible for the fundamental mode, yet is significant for the 2<sup>nd</sup> mode.

Mode	Shake / Weights	Resonance Peak, Hz	Normalised Displ.	% Roof : Basement
East-West 1	EW / Full	1.11	200(EW)	<b>3%</b>
	EW / 2x2	1.14		
North-South 1	NS / Full	1.64	80(EW)	<b>30%</b>
	NS / 2x2	1.67		
Torsion 1	EW / 2x2	2.38	25(NS)	<b>2%</b>
	NS / Full	2.35	5(NS)	
	NS / 2x2	2.38	5(NS)	
East-West 2	EW / None	4.53	2(EW)	<b>1%</b>
North-South 2	NS / None	7.22	0.8(NS)	<b>-21%</b>
Torsion 2	EW / None	6.57	0.4(EW), 0.20(NS)	<b>23%</b>
	NS / None	6.50	0.5(NS)	
East-West 3	EW / None	7.83	0.6(EW)	<b>0%</b>

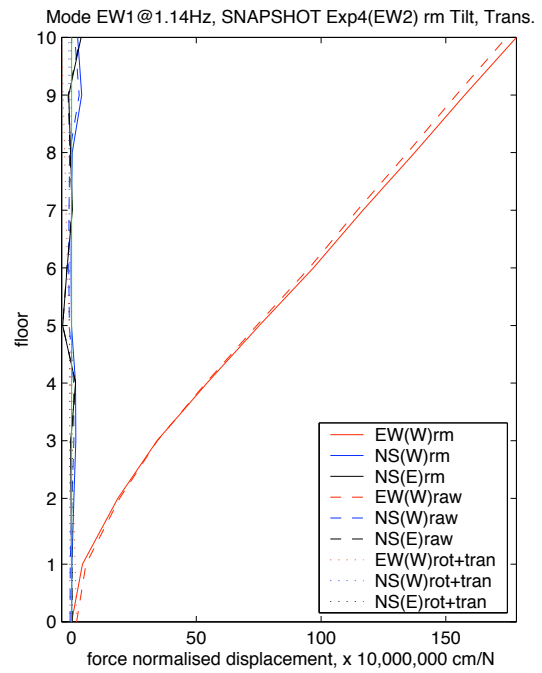
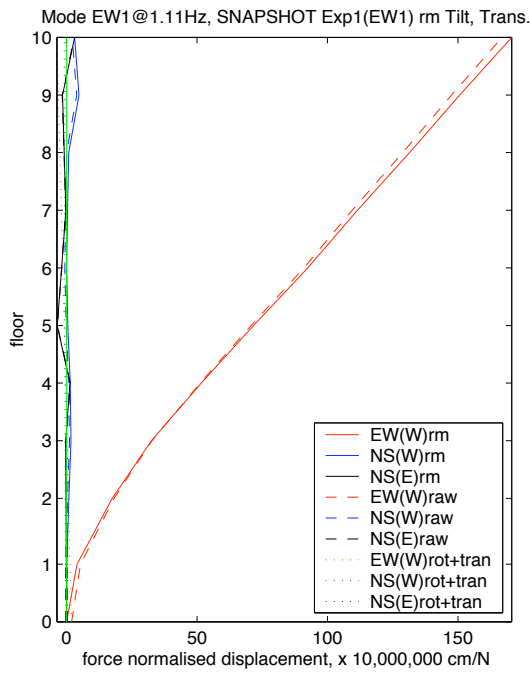
Table C.1: Millikan Library forced vibration results

Plots of the important modeshapes follow. More discussion of their shape, and comparison with theoretical modeshapes for homogeneous shear and bending beams, is in (Bradford et al, 2004).



(a) Full weights resonance curve

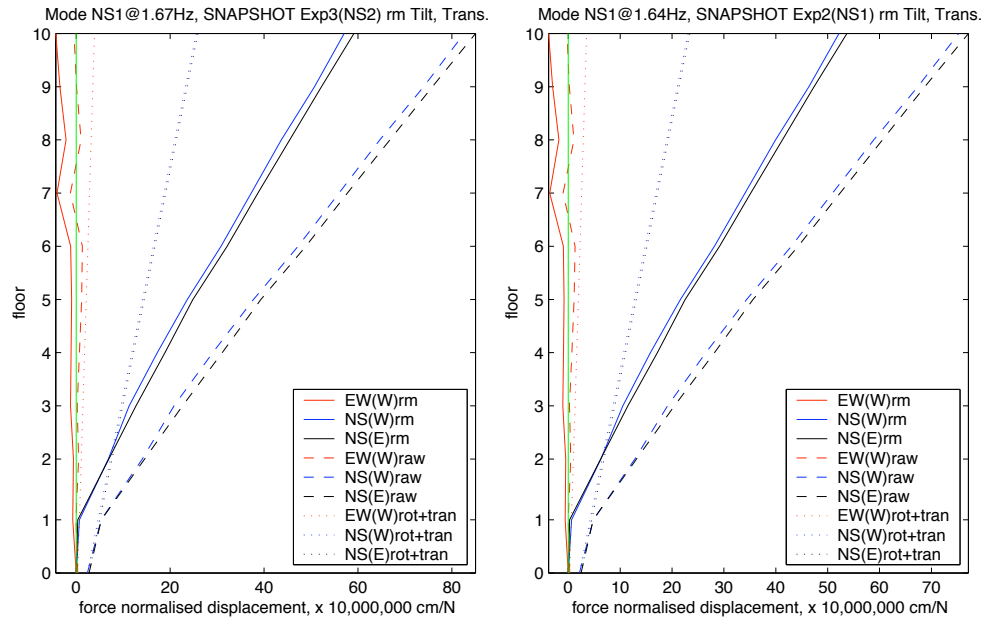
(b) 2x2 weights resonance curve



(c) Full weights - 1.11Hz

(d) 2x2 weights - 1.14Hz

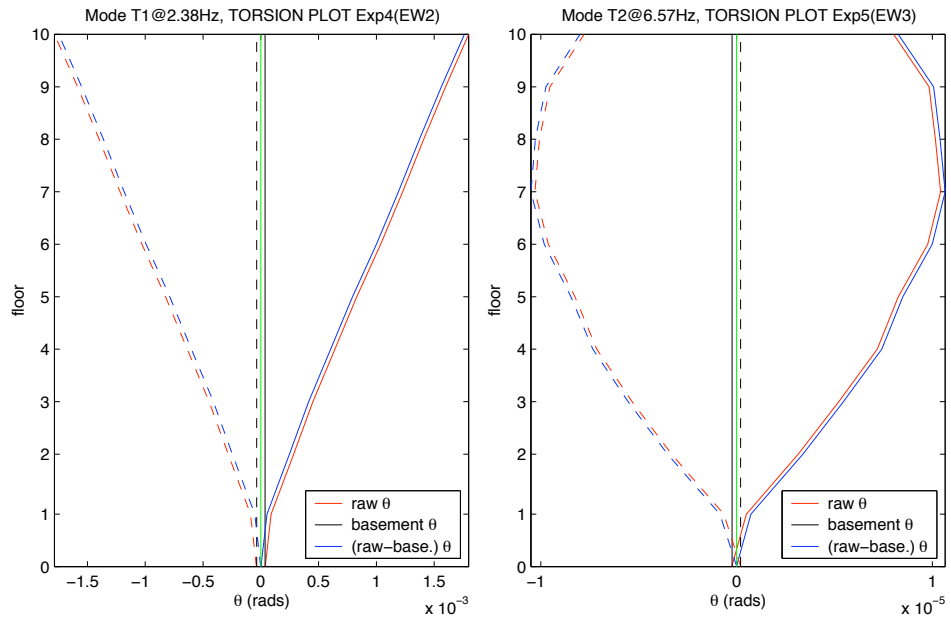
Figure C.3: Modeshapes and resonance curves for EW 1 Mode. Note shortening of natural frequency when loading increased.



(a) Full weights -  $1.67Hz$

(b) 2x2 weights -  $1.67Hz$

Figure C.4: Modeshapes for NS 1 mode. Note shortening of natural frequency when loading increased.

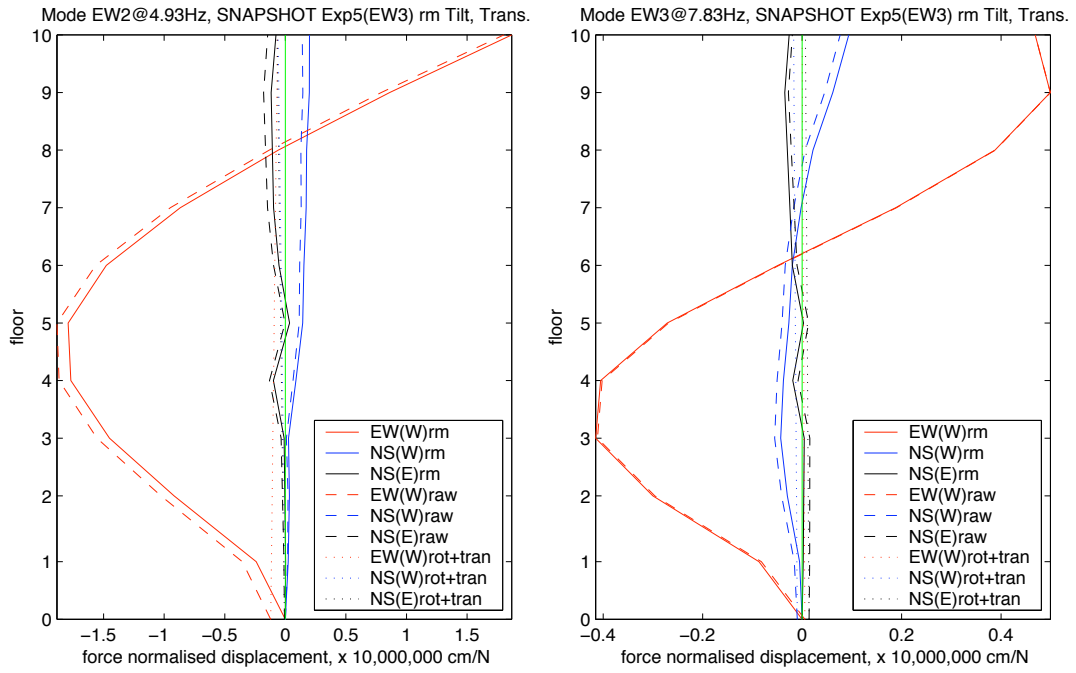


(a) Torsion 1 -  $2.37Hz$

(b) Torsion 2 -  $6.57Hz$

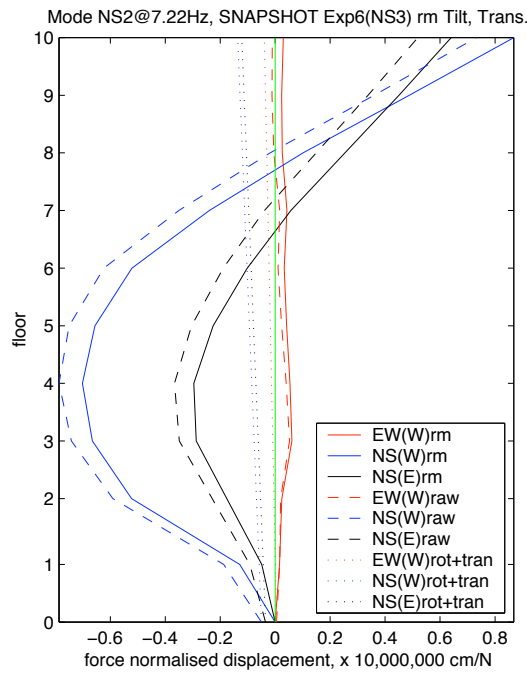
Figure C.5: Modeshapes for Torsion 1 and 2 modes





(a) EW 2 - 4.93Hz

(b) EW 3 - 7.83Hz



(c) NS 2 - 7.22Hz

Figure C.6: Modeshapes from higher-order modes - EW 2, EW 3, NS 2.